2nd International Conference for Groundwater Level Control Inside Cities, Nov., 7-8, 1999, Mansoura University, Egypt. Pp 72-88.

Solute Transport in Homogeneous and Heterogeneous Media: Comparison between Laboratory Experiments and Deterministic versus Stochastic Numerical Simulations

A.M.M. ELFEKI*
G.J.M. UFFINK
Faculty of Civil Engineering and Geo-sciences,
Delft University of Technology,
P.O. Box 5028, 2600 GA Delft, The Netherlands.

Abstract: Groundwater levels in urban areas are influenced by many factors. One of these factors is the leakage from sewerage systems, industry wastes and leaking pipelines. This leakage does not only influence the water levels, but it has also a strong impact on the groundwater quality. This paper focuses on the groundwater quality rather than the groundwater levels. In this paper, the influence of subsurface heterogeneity on the spreading of the contaminants that are released to the groundwater system is addressed.

A laboratory study on solute transport in artificially homogeneous and heterogeneous media is carried out. The motivation of this study is to get insight into the influence of heterogeneity on the phenomenon of dispersion and to distinguish the various dispersion regimes. The experiments are performed in a Prespex box filled with glass beads with different sizes to construct heterogeneous structures. Potassium Permanganate solution is used as an optical tracer and injected under steady state flow conditions. Analysis of the experimental results with some numerical deterministic and stochastic simulations is performed. The laboratory experiments and the numerical simulations demonstrate the influence of the presence of preferred pathways, the medium contrasts, the initial plume size and the spatial arrangements of the less and high permeable zones on the dispersion characteristics.

1. Introduction

For the simulation of groundwater contaminant transport numerical models are the most appropriate tools, due to their great flexibility and relatively low costs. However, validation of the concepts upon which these models are based, data and measurements from field tests and laboratory experiments are needed. For the support of new modelling approaches, field data are scarce and in general not sufficiently detailed. A physical model has been built for studying groundwater solute transport in artificial homogeneous and heterogeneous porous media. This model provides us with laboratory controlled conditions for a better understanding of the transport mechanisms in heterogeneous media. The motivation of these experiments is to get insight into the influence of heterogeneity on the phenomenon of dispersion and to distinguish the various dispersion regimes. Experimental studies of solute movement in saturated homogeneous media (column experiments) have been carried out since Bear [1961a]. However, multi-dimensional laboratory experiments in heterogeneous media have not been given much attention. The results of the laboratory experiments are compared with results predicted using deterministic and stochastic numerical models.

2. Experimental Set-up

The set-up consists of a box constructed from 1.2 cm thick Perspex sheets and filled with unconsolidated glass beads. The box is considered to represent a two-dimensional cross section of a confined aquifer with a limited third dimension. The inside dimensions of the working section of the box are 100 cm long, 56 cm wide, and 1 cm deep (see Figure 1). The ends of the box consist of two constant head tanks that are separated from the glass beads chamber by glass-fibber filters to keep the glass beads out of the head tanks. Influent and effluent reservoirs are connected to the constant head tanks by tubes. A pump is used at the influent tank for circulating the water in the system. The pump is capable of delivering a maximum of 6 l/min. By manipulating the water level in the inflow and

* on leave from Faculty of Engineering, Mansoura University, Egypt

outflow tanks different horizontal discharge rates and Darcy's fluxes can be establishedand a uniform groundwater flow field is obtained.

3. Porous Media and Method of Packing

Different-sized pure silica glass beads are selected and used to model the heterogeneity. Table 1 shows the size range and the average diameter, d_m, of the glass beads. The box is filled with one size of beads in case of a homogeneous sample. In case of heterogeneous samples, the box is filled with different sized beads. The filling and packing technique is as follows. Before packing, the beads are soaked in distilled water, washed and dried in 110^oC oven to remove any impurities due to manufacture. The model is filled partially with distilled water. Then, the beads are filled from the top into the model by a funnel. During the filling process, the model walls are blown by a hammer. Packing is guided by pre-designed arrangement of the media, to produce a heterogeneous porous medium with appropriate configuration. The porous medium rests directly against the bottom and sides of the model. From the top a strip of sponge rubber confines the top. The sponge rubber prevents any flow short-circuiting along the top of the medium. In case of heterogeneous samples, some filter rules should be followed to avoid segregation at the interfaces (the small sized grains fill the pores of the big sized ones). Some segregation, however, cannot be avoided during packing, especially for the very fine glass beads. Three different packing are selected and used for presentation here. The first is a homogeneous, the second contains block-shaped heterogeneity (it is called medium 1 in the text) and the third is packed in a form of perfect and imperfect horizontal layers (it is called medium 2). Medium 1 and 2 are shown in Figure 2.

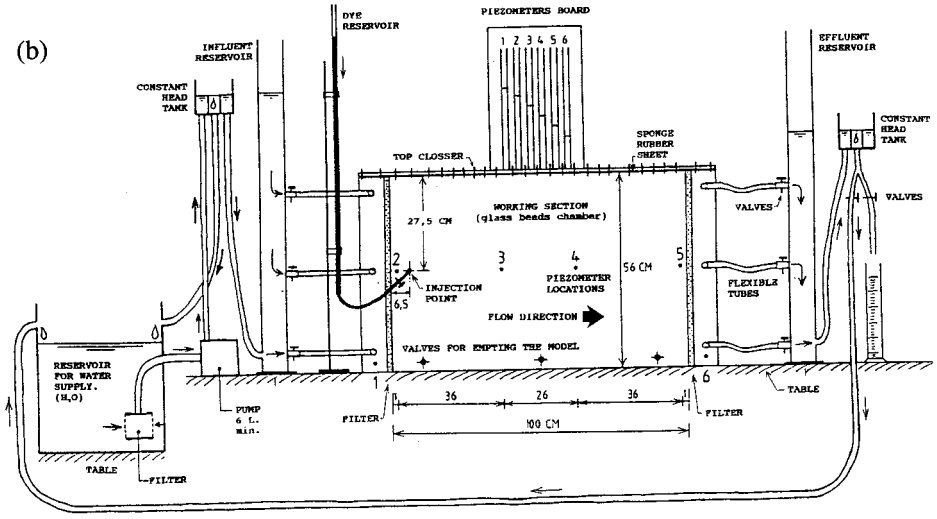

Figure 1. Experimental set-up.

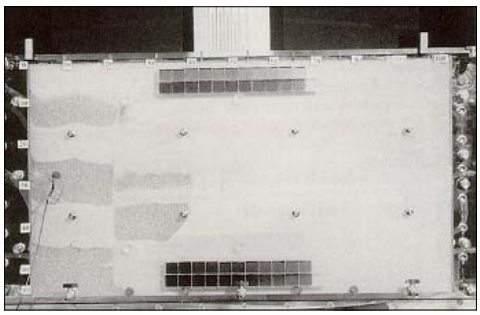

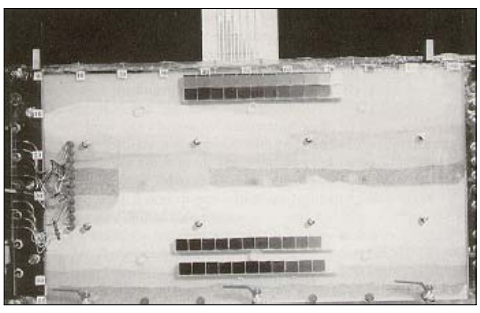

Figure 2. Glass beads box filled with two different heterogeneous structures. The left image is medium 1 and the right image is medium 2.

Table 1. Physical Parameters of the Glass Beads

	d_m (mm)	Measured K (cm/sec)		Empirical K (cm/sec)		α_l (mm)
		Loose	Dense	Hazen	Kozeny-Carman	
0.08 - 0.11	0.095	0.0064	0.0046	0.009	0.008	0.018
0.40 - 0.52	0.460	0.314	0.125	0.212	0.186	0.353
0.85 - 1.23	1.040	1.09	0.66	1.080	0.953	0.800
2.0 ± 0.5	2.00	2.08	1.93	4.00	3.52	1.405

4. Tracer

Potassium Permanganate ($KMnO_4$) solution is used as an optical tracer (dye). It is practically non-reactive. The tracer is injected instantaneously as a pulse through a 1mm hole at a distance of 27.5 cm from the top left corner of the model at the upstream side (6.5 cm from the inflow side). The tracer is introduced via a reservoir connected to the set-up by a plastic tube (see Figure 1). The evolution of the plume is monitored photographically at regular intervals.

5. Estimation of Media Properties

5.1 Estimation of Permeability

Constant head column experiments are performed to estimate the hydraulic conductivity of the glass beads. The hydraulic conductivity of the various beads is shown in Table 1 for dense and loose packing. The hydraulic conductivity value of each glass beads represents the mean over three column experiments per sample. Empirical values are estimated using Hazen formula and Kozeny-Carman equation (Bear, 1972). The empirical values reasonably match the measurements (see Table 1).

5.2 Estimation of Porosity

The real velocity, V, is related to the specific discharge, q, by the effective porosity, ε as,

$$V = \frac{q}{\varepsilon} \tag{1}$$

The effective porosity of beads (d_m=0.46 mm) is estimated by recording the plume centroid at regular intervals and plotting it as shown in Figure 2 (left graph). A best-fit line is plotted to the experimental data. The slope of the line corresponds to the real velocity as,

$$V = \frac{d\langle X \rangle}{dt} \tag{2}$$

where, $\langle X \rangle$ is the centroid displacement of the plume from the injection point and t is the corresponding time.
The specific discharge is calculated by the volume of water collected within a certain period of time, Q, divided by the cross-sectional area perpendicular to the flow direction as,

$$q = \frac{Q}{B\,D} \tag{3}$$

where, B is the model depth (56 cm) and D is the model thickness perpendicular to the flow direction (1 cm). From the experiment the effective porosity of (d_m=0.46 mm) is estimated to be about 40%.

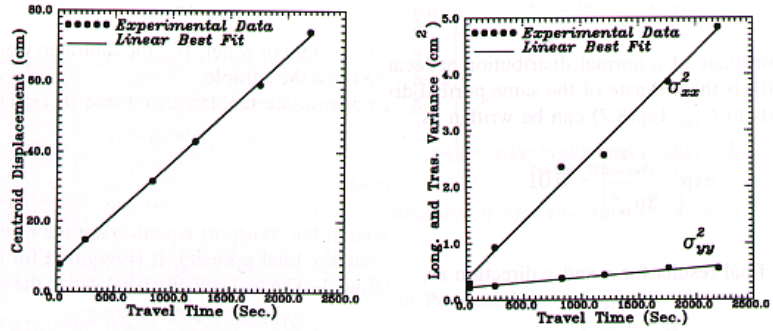

Figure 3. Estimation of parameters (left graph for porosity and right graph for dispersivity).

5.3 Estimation of Dispersivity

An approximate method is suggested to estimate dispersivity of beads size (0.40-0.52mm). The method is reliable in the beginning where the plume can be observed clearly. The method is based on measuring roughly the plume outline, which is elliptic in shape with maximum length, l_{xx}, and maximum width, l_{yy}, at specified times (see Figure 4). These dimensions are based on the visual concentration at the plume edges, C_e. C_e is assumed to be equal to 0.01 C_{max} where, C_{max} is the maximum concentration at the plume centre. The concentration field in homogeneous medium is known to be Gaussian. According to these assumptions one can write,

$$C_e = 0.01\,C_{\max} \tag{4}$$

where, C_e is the ordinate of Gaussian distribution at location $l_{xx}/2$ from the centre and C_{max} is the ordinate of the same Gaussian distribution at the centre.

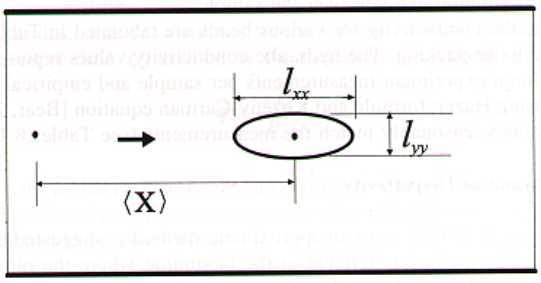

Figure 4. Plume Dimensions and Estimation of Dispersivities.

Eq. 4 can be written in a form of Gaussian distribution as,

$$\exp\left[-\frac{l_{xx}^{\,2}}{8\,\sigma_{xx}^{\,2}}\right] = 0.01 \tag{5}$$

With some manipulations, one can get a relation between the plume dimensions and the standard deviation of the

concentration distribution as,

$$\sigma_{xx} = \frac{1}{6} l_{xx} \quad , \quad \sigma_{yy} = \frac{1}{6} l_{yy} \tag{6}$$

The values of σ_{xx}^2 and σ_{yy}^2 are plotted versus travel time in Figure 3 (left). Using the linear best fitting techniques, the slope of the line corresponds to two times the dispersion coefficient (Dagan, 1989),

$$2 D_{xx} = \frac{d \sigma^2_{xx}}{dt} \quad , \; 2 D_{yy} = \frac{d \sigma^2_{yy}}{dt} \tag{7}$$

The dispersivities are calculated as,

$$\alpha_l = \frac{D_{xx}}{V}, \quad \alpha_t = \frac{D_{yy}}{V} \tag{8}$$

where, α_l is the longitudinal dispersivity, α_t is the transverse dispersivity and V is the mean real velocity given by,

$$V = \frac{K}{\varepsilon} J \tag{9}$$

where, J is the hydraulic gradient.
This method produces dispersivities α_l=0.333 mm and α_t=0.028 mm for beads size (0.40-0.52mm). The results of the method have been compared with the formula developed by Harleman, et al. (1963). The formula reads,

$$\frac{D_{xx}}{\nu_w} = \xi \, R_k^{\beta} \tag{10}$$

where, ξ is an empirical parameter which is 88 for sand grains, and 54 for medium composed of spheres (as in the current case), β is an exponent which is 1.2 for all cases, ν_w is the kinematic viscosity of water, and R_k is the Reynolds number of intrinsic permeability defined as,

$$R_k = \frac{V \sqrt{k}}{\nu_w} \tag{11}$$

The intrinsic permeability k is related to the conductivity K by,

$$K = \frac{k \, \rho_w \, g}{\mu_w} \tag{12}$$

where, μ_w is the dynamic viscosity of the water, ρ_w density of water and g is the gravitational acceleration equal to

9.81 ms^{-2}.
Form Eq.10, Eq.11 and Eq.12 one obtains the relation between K and α_l, and consequently the transverse dispersivity, α_t, is taken as one tenth of the longitudinal one,

$$\alpha_l = \xi V^{\beta-1} K^{\beta/2} \nu_w^{1-\beta/2} g^{-\beta/2}$$
$$\alpha_t = \frac{\alpha_l}{10} \tag{13}$$

Estimation of dispersivities by Eq.13 is tabulated in Table 1. One may notice that for d_m=0.46 mm the value of α_l obtained with Eq.13 (0.353 mm) is in the same order of magnitude as the value obtained from the visual method described here (0.333 mm). This agreement gives confidence in the formula developed by Harleman, et al. (1963). Therefore, it has been used to estimate dispersivities of the other glass beads and the results are displayed in Table 1.

6. Experimental Programme

In each test run, the set-up is packed and sealed. Flow is introduced by imposing a certain gradient on the model. After a steady state condition is established, a volume of dye is injected. The plume is monitored Photographically. Analysis of the experimental measurements (i.e. piezometric heads, the volume of the injected dye, plume centroid, plume dimensions, and the time of each snapshot) and the photographs are made. The experiments are run with initial concentrations, C_o, ranging from 0.00316 gram/cm^3 to 0.0104 gram/cm^3 $KMnO_4$.

7. Procedure for Numerical Simulations

Numerical simulations have been carried out to analyse the transport behaviour. The simulations are performed using computer models developed in this study. The simulation steps are:

1) *Schematzation:* The heterogeneous medium 1 and medium 2 shown in Figure 2 are schematized and displayed in Figure 7 (top row).
2) *Discretization and Parameter Assignation:* The homogeneous medium is discretized with gridsize 1 × 1 cm. For the heterogeneous media, a mesh of 2.5 × 1cm is used. The parameters of each glass bead are assigned according to Table 1. An average conductivity of the loose and dense values is applied. Local dispersivities are estimated using Eq.13. Porosity is assumed constant at 40%.
3) *Boundary and Initial Conditions:* The boundary conditions are constant head boundary at left and right sides of the flow domain. These heads are measured by piezometers number 2 and number 5 for left and right boundary respectively (see Figure 1). No-flow boundaries are assigned to the top and the bottom of the model. For the initial condition of the transport problem, an instantaneous injection is proposed from a single point as shown in Figure 2 (left image) or from multiple-points as in Figure 2 (right image).
4) *Flow Simulator:* The flow problem of each test is solved in terms of the hydraulic heads by the finite difference method. The hydraulic heads are checked with measured heads at some locations. The results are presented in Table 2. Good agreements are observed between the experimental results and the simulated ones.
5) *Transport Simulator:* The two-dimensional equation that describes solute transport taking into account advection, dispersion and diffusion, can be written in the following form (Bear, 1972),

$$\frac{\partial C}{\partial t} + V_x \frac{\partial C}{\partial x} + V_y \frac{\partial C}{\partial y} - \frac{\partial}{\partial x}\left[D_{d,xx} \frac{\partial C}{\partial x} + D_{d,xy} \frac{\partial C}{\partial y} \right] - \frac{\partial}{\partial y}\left[D_{d,yx} \frac{\partial C}{\partial x} + D_{d,yy} \frac{\partial C}{\partial y} \right] = 0 \tag{14}$$

where, C is the concentration field at time t, V_x and V_y are the components of the Eulerian velocity field in x and y direction respectively defined as follows,

$$V_y = -\frac{K}{\varepsilon}\frac{\partial \Phi}{\partial y} \tag{15}$$

$$V_x = -\frac{K}{\varepsilon}\frac{\partial \Phi}{\partial x} \tag{16}$$

where, ε is the effective porosity, K is the isotropic hydraulic conductivity, Φ is the hydraulic head, $D_{d,xx}$, $D_{d,xy}$, $D_{d,yx}$ and $D_{d,yy}$ are components of pore scale (micro-level) dispersion tensor (Bear, 1972),

$$D_{d,ij} = (\alpha_t |V| + D_m)\delta_{ij} + (\alpha_l - \alpha_t)\frac{V_i V_j}{|V|}, \qquad i,j = 1,2 \tag{17}$$

where, δ_{ij} is the Kronecker delta, δ_{ij}=1 for i=j and δ_{ij}=0 otherwise, α_l is the longitudinal dispersivity, α_t is the transversal dispersivity, D_m is the molecular diffusion coefficient, the indices 1 and 2 correspond to x and y directions respectively and $|V|$ is the magnitude of the resultant velocity given by $|V| = \sqrt{V_x^2 + V_y^2}$.

The particle tracking random walk method (Uffink, 1990) is used to solve Eq. 14 numerically. The x-coordinate of the particle displacement is calculated by,

$$\begin{aligned} X_p(t+\Delta t) = X_p(t) \; + \; & V_x(X_p(t), Y_p(t))\Delta t + \\ & \left(\frac{\partial D_{d,xx}}{\partial x} + \frac{\partial D_{d,xy}}{\partial y}\right)\Delta t + \\ \frac{V_x}{|V|}\, Z\sqrt{2\alpha_l\, |V(X_p(t), Y_p(t))|\Delta t} & - \frac{V_y}{|V|}\, Z'\sqrt{2\alpha_t\, |V(X_p(t), Y_p(t))|\Delta t} \end{aligned} \tag{18}$$

where, $X_p(t)$ is the x-coordinate of a particle at time t, $X_p(t+\Delta t)$ is the x-coordinate of a particle at time $t+\Delta t$, Δt is the time step of the calculations, Z, Z' are two independent random numbers drawn from normal distribution with zero mean and unit variance. The terms between brackets are called the Fokker Plank terms (Uffink, 1990). Similarly, the y-coordinate can be calculated.

8. Simulation Results and Discussion

8.1 Deterministic Simulations

Deterministic simulations have been performed to validate the numerical models developed in this study. In these simulations, the heterogeneous structure and the permeability values are assumed to be known with certainty.

i) Homogeneous Medium

The results of the tests in case of homogeneous medium are displayed in Figure 5 and 6. Figure 5 shows snapshots of the plume at different times. The numerical simulation matches the experimental observations reasonably well. The movement of the centroid of the plume and the longitudinal and transverse variances are presented in Figure 6. Numerical simulations are performed with the dispersivities calculated by the suggested visual method and the results are pretty good.

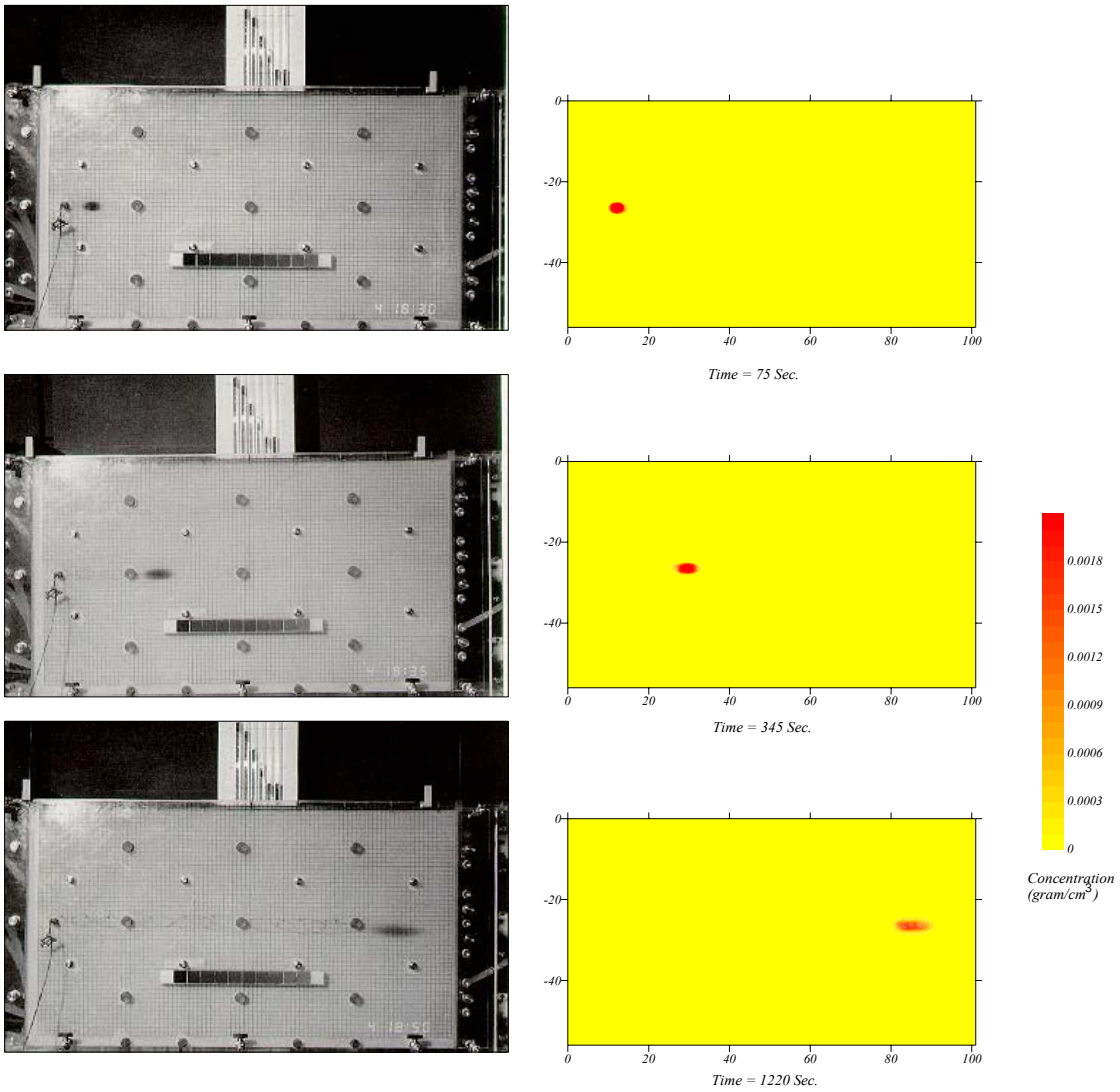

Figure 5. Numerical simulation of the tracer injection in homogeneous medium (left column is the experiments and right column is the corresponding numerical simulations).

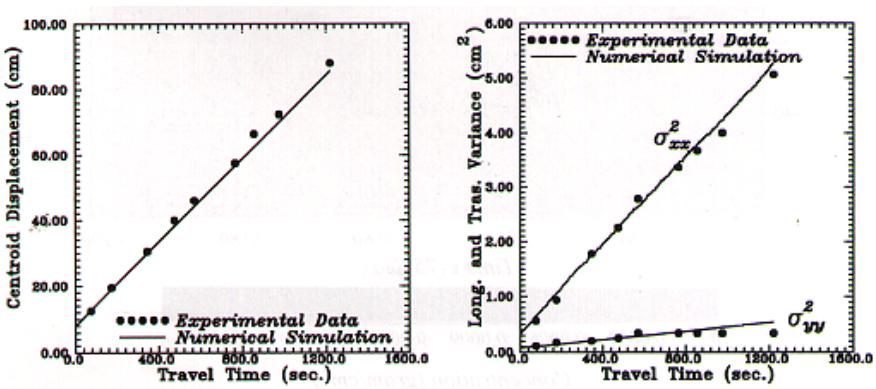

Figure 6. Plume spatial moments in homogeneous field (left: 1st moment, certroid displacement, right: 2nd moment, spreading around the certroid).

Table 2. Measured and Simulated Hydraulic Heads in the Experiments.

Piezometer Figure 1	Location from the left edge (cm)	Measured Head (cm)	Simulated Head (cm)
		Homogeneous Medium.	
No. 3	X = 36.8	44.10	44.14
No. 4	X = 63.5	40.50	40.40
		Heterogeneous Medium1	
No. 3	X = 36.8	47.00	46.75
No. 4	X = 63.5	40.80	40.90
		Heterogeneous Medium2	
No. 3	X = 36.8	40.80	40.40
No. 4	X = 63.5	38.60	38.20

ii) Heterogeneous Media

The experimental tests and their corresponding numerical simulations are shown in Figure 8, 9 and Figure 10, 11 for medium 1 and 2 respectively.

- *Heterogeneous Medium 1 with Single Point Instantaneous Injection*: The flow results show good agreements in terms of the hydraulic heads at the selected piezometers as shown in Table 2. Figure 8 (2nd row) shows three snapshots of the simulated solute plumes at certain intervals. The overall comparison between the laboratory tests and the numerical simulation is satisfactory. The highest concentrations occur in the middle part, while the outer edges are more diluted. Figure 9 shows the plume statistics. It is clear from the numerical simulations that the centroid displacement is linear, and the breakthrough curves display Gaussian characteristics. However, the spreading of the plume shows non-Fickian behaviour. One may recognize that the longitudinal dispersion is decreasing. This behaviour is due to the fact that the plume size is small with respect to the the size of the heterogeneous units. The plume movement is influenced by the spatial arrangements of the various glass beads while the spreading mechanisms are governed by the local dispersivities in each glass beads. Since the plume moves from a highly permeable zone near the source to less permeable zones therefore the spreading is high in the beginning. However, after some time the plume goes to zones of lower dispersion and consequently the spreading rate decreases which causes the longitudinal variance to grow slowly and subdiffusive regime occurs.

- *Heterogeneous Medium 2 with Multi-Points Instantaneous Injection*: Similar tests have been carried out for medium 2. The measured and simulated heads show also satisfactory agreement (see Table 2). Figure 10 (2nd row) shows snapshots of the simulated plume at different times since release. The results show general agreement in terms of plume shapes. Figure 11 displays the plume centroid, breakthrough curve, longitudinal and lateral variances and the macro-dispersion coefficients. The breakthrough curves show non-Gaussian behaviour due to the influence of low permeable zones where parts of the plume are trapped and take long time to get released to high permeable zones. The longitudinal variance shows a

superdiffusive regime at early times. However, at 250 seconds the plume seems to reach a dispersive regime. This behaviour can be attributed to the fact that the plume sampled all the heterogeneity in the system so the heterogeneity does not contribute any more in the spreading. Therefore Fickian regime is reached with (D_{xx} = 2.5 cm^2/sec). In heterogeneous medium 1 the breakthrough curve shows Gaussian behaviour. However, in heterogeneous medium 2 the breakthrough curve shows non-Gaussian behaviour. This means the breakthrough curve does not always reveal the real dispersive behaviour.

8.2 Stochastic Simulations

So far, deterministic simulations have been carried out to study the dispersion mechanisms in heterogeneous media. However in this section, some stochastic simulations are carried out. The idea behind these simulations is to estimate the uncertainty in the plume spreading due to the uncertainty in the heterogeneous structure which is often the case in field problems. Heterogeneity is often known at some sampled locations and away from these locations there will be uncertainties regarding the spatial structure. Stochastic realizations of the heterogeneous structures constructed in the experiments (i.e. medium 1 and medium 2) have been generated using the coupled Markov model developed by Elfeki et al. (1995). This technique has many applications (see e.g. Elfeki, et. al. 1996 and 1998). A short description is given below.

The coupled Markov chain method is a stochastic technique that couples two chains. The first one is used to describe the sequence of variation in lithology in the vertical direction and the second chain describes the sequence of variation in the horizontal direction. The two chains are coupled in the sense that, a state of a cell in the domain is dependent on the state of two cells the one on top and the other on the left of the current cell. This dependence is described in terms of transition probabilities from the two chains. This technique is efficient in terms of computer time and storage in comparison with other techniques available in the literature such as sequential indicator simulation, Markov random fields and truncated Gaussian method. Figure 7 (bottom row) shows realizations of the heterogeneous structures generated by the coupled Markov chain model.

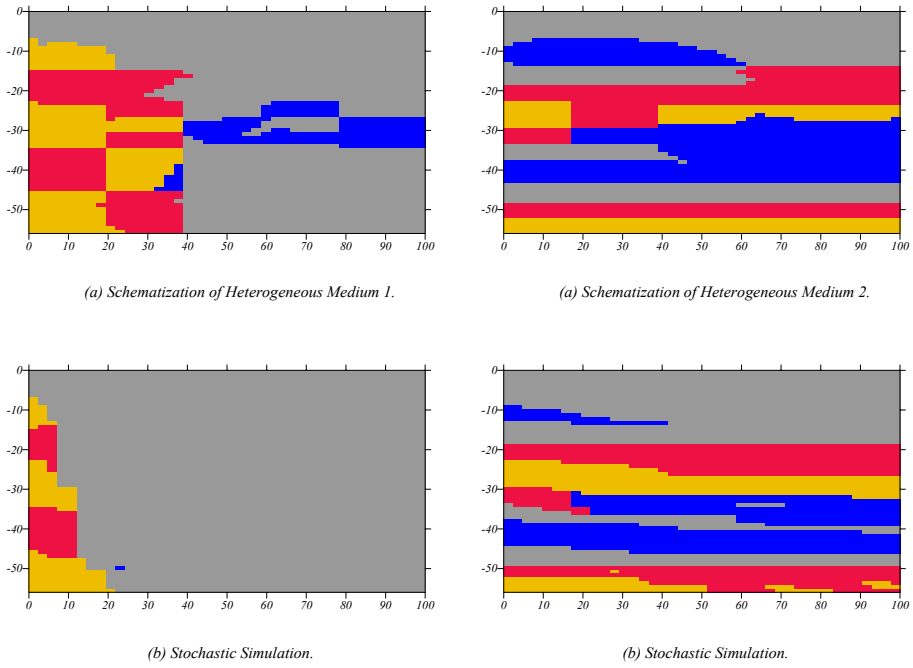

Figure 7. Schematic representation of the heterogeneous structures used in the experiments medium 1 and 2 (top row). Single realizations generated using the coupled Markov chain model, Elfeki, et al., 1995 (bottom row). Dark areas are low permeable and light areas are high permeable.

In the stochastic simulations, it is assumed that the arrangement of the heterogeneous units (glass beads) is known in terms of transition probabilities between these units. Figure 7 (top left) shows schematization of medium 1 and a single stochastic simulation is presented in the bottom left corner in the same figure. The right side of Figure 7 shows

a schematization of medium 2 (on the right top corner) and its corresponding stochastic simulation is displayed in the right bottom corner. Flow and transport equations have been solved in 100 realizations of these artificial structures. The ensemble concentration field and the standard deviation in the concentration field are calculated and displayed in Figure 8 (3rd and 4th rows) for medium 1 and in Figure 9 (3rd and 4th rows) for medium 2 respectively. In both cases, the ensemble concentrations show a wide spread over the region. This is due to the fact that there is a large degree of freedom in the variability from one realization to another. Considerable uncertainty in the concentration field is due to the wide range of variability among the realizations. It is noticeable that the real plume differs significantly from the ensemble plume. Therefore, the ensemble can only be used to provide the envelope where one can predict the plume location, however it is still difficult to quantify the uncertainty on the concentration values. The spatial moments of the real plume, the ensemble mean and 95% confidence intervals of the ensemble plume are shown in Figure 12 (left part is medium 1 and right part is medium 2). It is clear that the spatial moments fall in the 95% confidence intervals because the envelope of uncertainty is wide due to the high degree of uncertainty between the realizations. The only way to reduce this uncertainty is by performing conditional simulations. This point will be considered in the future research.

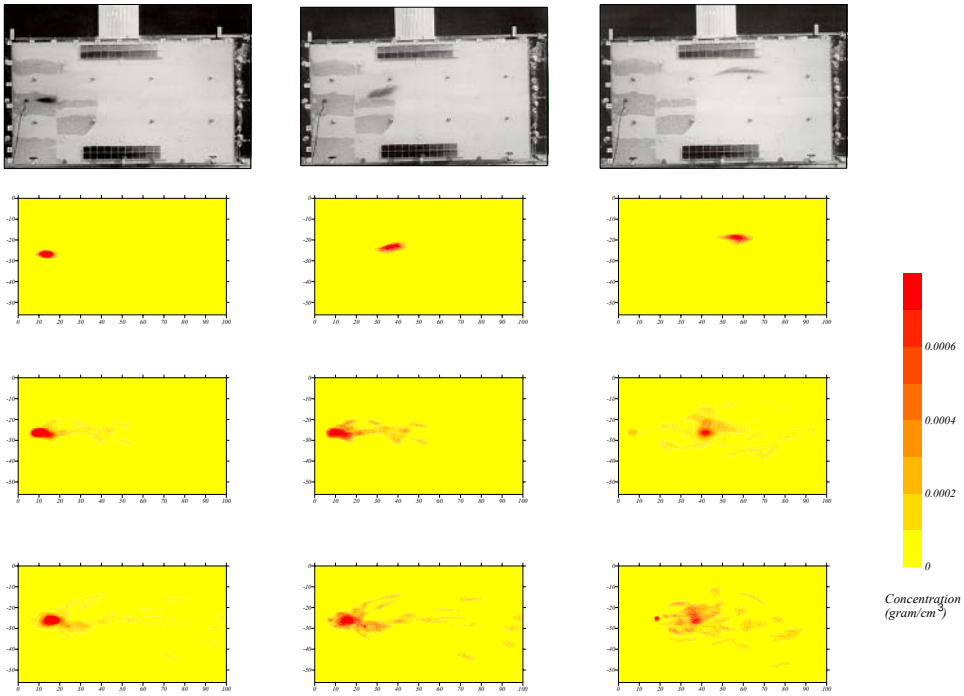

Figure 8. Deterministic and stochastic simulations of the experiments in the heterogeneous structure (medium 1). Top row is three snapshots of the plume at 60, 230 and 420 seconds respectively, 2nd row is the corresponding deterministic simulation, 3rd row is the ensemble average concentration field and bottom row is the standard deviation in the concentration field.

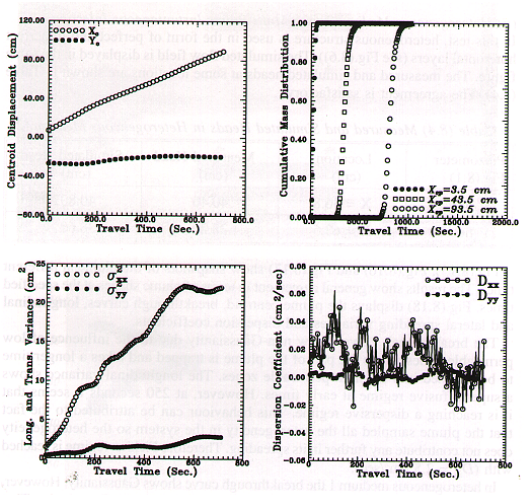

Figure 9. Spatial moments (left column), breakthrough curves (top right corner) and macro-dispersion (bottom right corner) coefficients of the plume in medium 1.

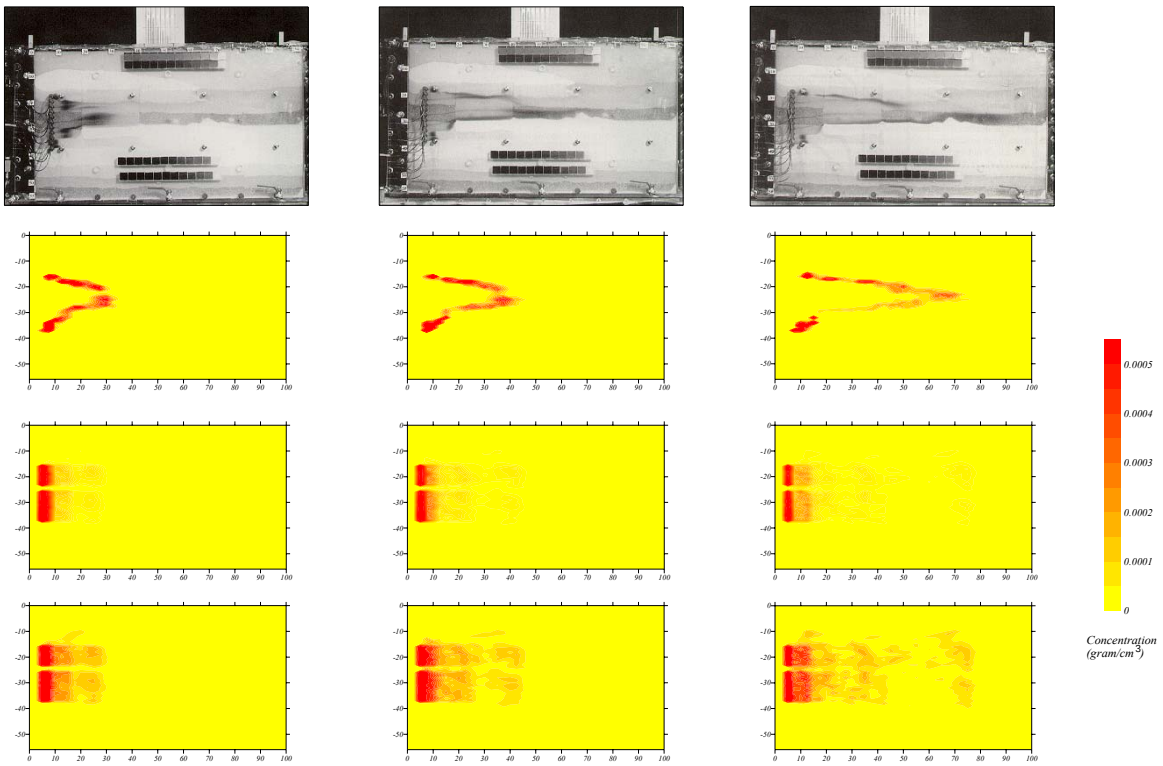

Figure 10. Deterministic and stochastic simulations of the experiments in heterogeneous structure (medium 2). Top row is three snap shots of the plume at 50, 90 and 170 seconds respectively, 2nd row is the corresponding deterministic simulation, 3rd row is the ensemble average concentration field and bottom row is the standard deviation in the concentration field.

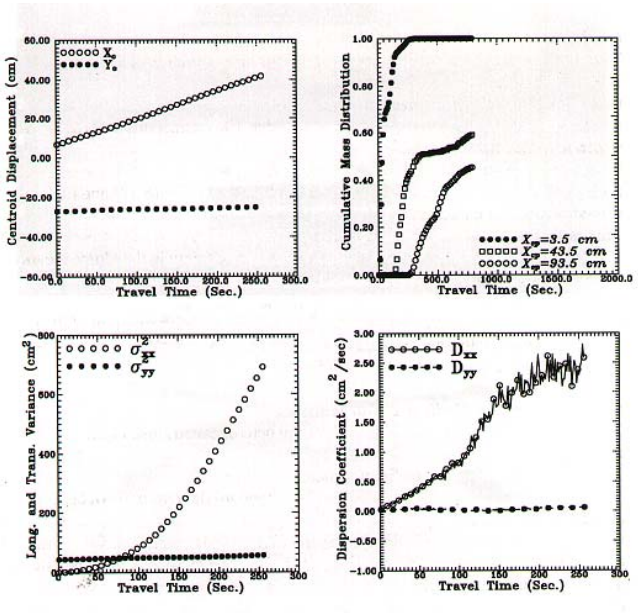

Figure 11. Spatial moments (left column), breakthrough curves (top right corner) and macro-dispersion coefficients (bottom right) of the plume in medium 2.

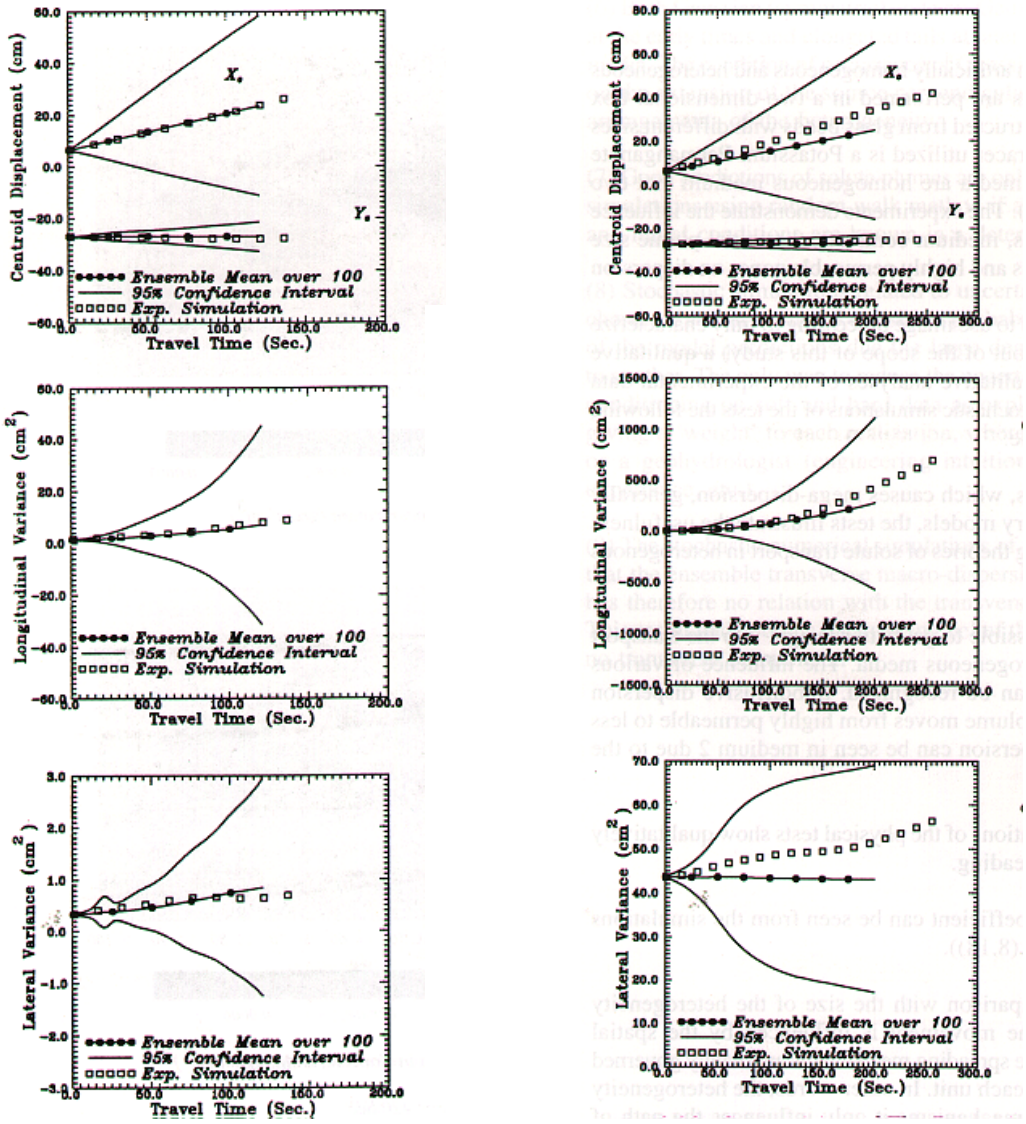

Figure 12. Uncertainty in spatial moments of the plumes (left column is medium 1 and right column is medium 2).

Conclusions

A laboratory study on solute transport in artificially homogeneous and heterogeneous media is carried out. The experiments are performed in a Prespex box filled with glass beads with different sizes to construct heterogeneous structures. Potassium Permanganate solution is used as an optical tracer and injected under steady state flow conditions. Analysis of the experimental results with some numerical deterministic and stochastic simulations is performed. The laboratory experiments and the numerical simulations demonstrate the influence of the presence of

preferred pathways, medium contrasts, the initial plume size and the spatial arrangements of the less and high permeable zones on the dispersion characteristics. From qualitative analyses of the experimental data and the corresponding numerical deterministic and stochastic simulations of the tests the following conclusions and remarks can be made,

1. Although the geological interfaces, which causes mega-dispersion, generally cannot be simulated easily in laboratory models, the tests illustrate the usefulness of controlled experiments in supporting theories of solute transport in heterogenous media (e.g. Non-Fickian theories).
2. The tests demonstrate that it is possible to get better insight into the transport behaviour in homogeneous and heterogeneous media. The influence of various interfaces on dispersion behaviour can be recognized. Subdiffusive dispersion is observed in medium 1 because the plume moves from high permeable to less permeable zones. Superdiffusive dispersion can be seen in medium 2 due to the existence of preferential flow paths.
3. The deterministic simulations of the experimental tests show qualitatively similar results in terms of plume shapes.
4. The scale-dependent dispersion coefficient can be seen from the simulations in heterogeneous medium 2.
5. When the plume is small in comparison with the size of the heterogeneity (heterogeneous medium 1) the plume movement is influenced by the spatial arrangements of the various units but the local dispersion process inside each unit governs the spreading mechanisms. In other words, the heterogeneity does not contribute in the spreading mechanisms it only influences the path of the plume.
6. Both Gaussian (symmetric) and non-Gaussian breakthrough curves (steep fronts at the early times and elongated tails at later times) can be found in the heterogeneous media. The condition of occurrence of Gaussian or non-Gaussian behaviour depends on the extension of the source perpendicular to the flow direction and the spatial arrangements of the heterogeneity.
7. Good predictions of the solute plumes are possible by performing deterministic simulations using random walk method if all details of the aquifer heterogeneity and initial conditions are known in a deterministic sense.
8. Stochastic simulations used for quantification of uncertainty show considerable uncertainty of the model predictions due the large degree of freedom from one realization to another. The only way to reduce the uncertainty in field applications is to perform conditioning. This point will be considered in future research.

References

Bear, J. (1961a). Some Experiments in Dispersion. *J. Geophys. Res*., 66(8), pp.2455-2467.

Bear, J. (1972). *Dynamics of Fluids in Porous Media.* American Elsevier, New York.

Dagan, G. (1989). *Flow and transport in Porous Formations*. Springer, Verlag, Berlin.

Elfeki, A. M. M. & Uffink, G. J. M. & Barends, F. B. J. (1995). Stochastic Simulation of Heterogeneous Geological Formations Using Soft Information, with An Application to Groundwater. In *Groundwater Quality: Remediation and Protection, QG'95*. Edited by Kovar, K. and Krasny, J..IAHS Publication No. 225, pp. 192-202.

Elfeki, A. M. M.& Uffink, G. J. M. & Barends, F. B. J. (1996). Solute Transport in Single and Multiple Scale Heterogeneous Formations: Numerical Experiments*, geoENV 96*, *First European Conference on Geostatistics for Environmental Applications,* Lisbon, Portugal. Ed. by A. Soares, J. Hernandez & R. Froidevaux. Kluwer Academic Pub.,pp. 51-63.

Elfeki, A. M. M.& Uffink, G. J. M. & Barends, F. B. J. (1998). A Coupled Markov Chain Model for Quantification of Uncertainty in Transport in Heterogeneous Formations. To appear in *geoENV 98*, *Second European Conference on Geostatistics for Environmental Applications,* (18-20 Nov., 1998), Valencia, Spain, Ed. by A. Soares, J. Hernandez Kluwer Academic Publishers.

Elfeki, A.M.M. (1996). *Stochastic Characterisation of Geological Heterogeneity and Its Impact on Groundwater Contaminant Transport.* Ph.D. Thesis. Delft University of Technology., Delft, The Netherrlands. A. A. Balkema Publishers, Rotterdam, The Netherlands.

Harleman, D. R. F. & Melhorn, P. F. & Rumer, R. R. (1963). Dispersion permeability correlation in Porous Media*. J. Hydraulics Div. ASCE*, 67-85.

Uffink, G.J.M. (1990). *Analysis of Dispersion by the Random Walk Method*. Ph.D. Thesis. Delft University of Technology, Delft, The Netherlands.

Acknowledgements

This paper has been written during the leave of the first author at Dept. of Applied Earth Sciences, Faculty of

Civil Engineering and Geo-sciences, Delft University of Technology, Delft, the Netherlands. Thanks are due to Prof. Ir. Cor Van Kruijsdijk and Dr. Hans Bruining for giving me the opportunity to present the paper in the conference during my work in the DIOC project (multi-scale stochastic modelling of subsurface heterogeneity).